Accepted manuscript doi:
10.1680/jgele.22.00067

Submitted: 27 June 2022

Published online in 'accepted manuscript' format: 30 September 2022

Manuscript title: Comparing laboratory and field samples of lime-cement improved Norwegian clay

Authors: P. Paniagua*, F. A. Falle[†], S. Hov[‡], K. R. Tekseth[§], F. Mirzaei[§] and D. W. Breiby[§]

Affiliations: *Geotechnics and Natural Hazards, Norwegian Geotechnical Institute & Geotechnical Division, Norwegian University of Science and Technology, Trondheim, Norway; [†]Geotechnical Division, Norwegian University of Science and Technology, Trondheim, Norway; [‡]Geotechnics and Natural Hazards, Norwegian Geotechnical Institute, Trondheim, Norway and [§]Department of Physics, Norwegian University of Science and Technology, Trondheim, Norway

Corresponding author: P. Paniagua, Geotechnics and Natural Hazards, Norwegian Geotechnical Institute & Geotechnical Division, Norwegian University of Science and Technology, Trondheim, Norway.

E-mail: priscilla.paniagua@ngi.no

Accepted manuscript doi:
10.1680/jgele.22.00067

Abstract

Improving the structural integrity of clay-rich soil is crucial to mitigate risks related to ground movements, and representative procedures are needed to quantitatively describe the reproducibility and authenticity of laboratory-mixed clay model specimens. Here, two standardised industry protocols for preparation of laboratory lime-cement improved clay samples are compared to field lime-cement improved clay. Samples from both dry deep mixed (DDM) clay columns and laboratory mixed clay, with different binder quantities, were tested for density, water content, unconfined compressive strength, and analysed by X-ray micro-computed tomography. Results showed clear differences in sample density and 'macro-porosity' described as entrapped air resulting from field installation and laboratory preparation (i.e., moulding technique). For the field samples, the macro-porosity was relatively low (< 2 %), indicating that the air used in the binder injection is successfully evacuated along the drilling rod as sought after during in-situ DDM works. For the laboratory samples, prepared with two standard moulding preparation protocols, the macro-porosity was larger and having an influence on the measured strength and stiffness of the improved soil. An inverse relation between the mechanical strength under unconfined compression and porosity was found. In conclusion, the industry-standard laboratory moulding techniques fail to reproduce specimens that are representative for field conditions.

Keywords: Ground improvement; Clays; Laboratory tests

Accepted manuscript doi:
10.1680/jgele.22.00067

Introduction

In the Nordic countries, in-situ improvement of strength and deformation properties of clayey soils with lime-cement (LC) is commonly done by the dry deep mixing (DDM) method (Kitazume & Terashi, 2013; Karlsrud et al., 2015; Larsson, 2021). The Nordic DDM is normally performed by drilling down to 20-23 m using a mixing tool of 0.6-0.8 m diameter and then feeding a dry binder by air pressure into the soil, while retrieving and rotating the tool towards the surface at a certain rate (NGF, 2012).

DDM works are usually combined with laboratory tests on laboratory mixed (LM) samples prepared with clay collected from the project site and the binder used in the field. Ideally, the strength development in laboratory and field conditions should be equal or similar, however, for the Nordic DDM method, the field strength is normally higher than the laboratory strength (Larsson, 2003; Karlsrud et al., 2015). The resulting shear strength development of an improved clay is a function of several factors such as type of soil; type and amount of binder (Åhnberg et al., 1995; Jacobson et al., 2003; Broms, 2004; Kitazume & Terashi, 2013); homogeneity, curing conditions and testing methods (Larsson et al., 2005; Åhnberg & Holm, 2009; Kitazume, 2015). The shear strength development for LM samples is also affected by the sample preparation itself, e.g., moulding technique and mixing time (e.g., Kitazume, 2005, 2012; Åhnberg & Holm, 2009; Kitazume et al., 2015).

In Norway, two moulding techniques have been developed for preparing LM samples: the SVV-technique (SVV, 2016) and the NGF-technique (NGF, 2012). Both methods involve similar steps, however, the clay-binder mixture often has poor workability due to i) an immediate hydration reaction between the soil pore water and the binder, and ii) flocculation/agglomeration due to cation exchange. This reaction results in the creation of pore networks inside the samples, which affect the mixture compaction. By experience, the two methods tend to create samples with different macro-scale mechanical properties, even though both methods should ideally give similar results. Microstructural investigations can reveal the inner interactions between the soil and added binders and explain these differences (Jian et al. 2016). Non-invasive laboratory methods have recently been applied to describe the role of porosity on the mechanical behaviour of treated soils (Bellato et al., 2020). For example, by using X-ray micro computed-tomography (μCT) it is possible to investigate the microstructure of materials and estimate the resolved porosity within a soil sample (Viggiani & Hall, 2012). μCT is a technique that exploits spatial variations in a material's X-ray attenuation coefficient allowing a 3D reconstruction of a sample by back projecting a stack of unique X-ray shadow projections obtained at different sample orientations using a mathematical algorithm (Cnudde & Boone, 2013). The μCT microscopy technique is still not

widespread in the analysis of clay-binder mixtures, despite increasing use in related fields, see e.g., Chavez Panduro et al. (2020).

This work studies the Nordic DDM method by comparing field mixed (FM) and LM samples (processed using two moulding techniques) of a clay in order to define which method best reproduces field properties. The study involves geotechnical characterisation and μCT (Falle, 2021) of LC improved field and laboratory clay samples. This microstructural study helps to qualitatively understand the differences caused by mixing under both conditions.

Materials and methods

Holvegen clay from Skatval, Norway, is a low plasticity silty clay with water content near 30%, unit weight of 19-20 kN/m³, unconfined compressive strength of 18-20 kPa and remoulded shear strength of 6 kPa. The clay strength was improved using a 50/50 dry weight ratio of lime/cement. A lime containing > 75% active calcium oxide (CaO) and a standard Portland type CEM II were used.

The DDM works at Holvegen included columns with α varying between 30-80 kg/m³, see Table 1. These α values are lower than the standard values (80-100 kg/m^3) recommended by NGF (2012). This low binder content challenges the installation of LC columns (Hov et al. 2022) due to equipment issues relating to binder delivery. Therefore, the retrieval rate was increased to maintain the homogeneity of the LC columns, to give a better contact between the binder and the soil particles, and thus a higher reaction rate and faster temperature development (Kitazume & Terashi, 2013). All columns were produced using an 8-blade Ø800 mm mixing tool to a target depth of 10-15 m, using a binder injection pressure of 4-7 bars.

About 8-10 samples of 3-8 kg from 5 m depth were taken after 21 and 63 days of installation. The samples were trimmed to Ø54 mm and 100 mm height cylinders and stored at room temperature (Bache et al., 2021), until they were tested after 28 days and 70 days, respectively, of curing since installation.

For LM samples, Holvegen clay was mixed with LC with the same α as used in the field. Cylindrical samples of Ø54 mm and 100 mm height were moulded using either the NGF-technique or SVV-technique, see Table 2. The NGF-technique is a dynamic compaction method where the LC clay is placed in layers of 20 mm thickness and each layer is compacted by a brass cylinder or rod of 1200 g with Ø20 mm. Norwegian Geotechnical Society, NGF (2012), specifies that the impact energy should be 0.2–0.25 Newton-meter (Nm) per blow and that this should be applied 20 times per layer. The SVV-technique is a static compaction method using air pressure, where LC clay is placed in 20 mm-thick layers and each layer is compressed by 200 kPa of pressure until the

full height of 100 mm is reached, i.e., mixture is compacted in a total of 5 layers. The static pressure is held for 10 s and is usually applied with an air-pressure apparatus attached with a piston with a diameter slightly less than the specimen diameter to allow evacuation of air. After the moulding, the LM samples were cured for 28 days at room temperature.

FM and LM samples were tested in unconfined compression (UC) tests (ASTM D2166-06, *Standard Test Method for Unconfined Compressive Strength of Cohesive Soil*). Three samples of each LM combination and five samples of each FM combination were tested to ensure repeatability of the results. The deformation rate was set to 1.5% strain/minute. The shear strength, denoted τ_{max}, was interpreted as half of the maximum vertical stress at failure (q_{uf}), i.e., $\tau_{max,\ 28\ d} = q_{uf}/2$.

Full size FM and LM samples were scanned by µCT (see Table 3) using a Nikon XT H 225 ST instrument equipped with a 16-bit Perkin Elmer 1620 X-ray detector that has a 200 µm pixel size and a field of view of 400x400 mm^2 (2000x2000 pixels). All scans were conducted using a high tube voltage (> 200 kV) to obtain a decent signal through the samples with a resulting focal spot size of about 25 µm. Setup parameters for the apparatus were adjusted to find the optimum values giving a decent signal, contrast, and image resolution. Three-dimensional samples were reconstructed using Nikons proprietary reconstruction software that utilizes the Feldkamp-Davis-Kress algorithm with a Ram-Lak filter (Feldkamp et al. 1984). A slow spatial density variation, a so-called "X-ray anode heel artifact", extending axially through the reconstructed samples, was removed prior to further analysis. µCT allowed sample mapping showing differences in density, binder-clay layering, or any other discontinuity. The reconstructed volumes were filtered with an iterative non-local means filter (Bruns et al. 2017) and segmented by a manually set threshold value to separate pores from the main structure. A region of interest was selected inside each of the samples and further processed by a morphological closing that removed pores smaller than 2x2x2 voxels, eliminating pores that cannot be conclusively distinguished from noise.

Test results and discussion

Figure 1 shows cross sections of FM samples after UC tests. Samples with α = 30 kg/m³ seem to be affected by poor mixing, with pockets of non-disturbed clay surrounded by areas with binder. Table 4 presents the laboratory results of the tested FM samples. Samples with α = 50 kg/m³ give the highest strength due to the longest curing time. When translated to 28 days curing time, using the formula proposed by Åhnberg (2006), however, the strength is comparable to the samples with α = 80 kg/m³. For RIII-b samples, the strength is lower

than the RIII-a samples, maybe due to an inappropriate feeding and/or mixing of the binder in the specific section where the sample was obtained.

LM samples gave a large variation in material strength when changing α. The clay mixed with the highest α became stiffer and more difficult to compact. The moulding technique caused changes in the density of the samples: the NGF-technique created around 10% denser samples than the SVV-technique for all α (see Table 4). Compared to the corresponding field samples, the density values of the laboratory samples were relatively lower. In addition, an increasing the density, increased the strength of the samples. The NGF-technique on average yielded samples with 40-60% higher strength than the SVV-technique and tended to represent the field strength more successfully (see Figure 2a). The results (Figure 2b) support the hypothesis of an inverse linear relationship between strength and porosity, as observed by Bellato et al. (2020) for strength improved sand.

Figures 3, 4 and 5 show the 3D-images taken of the FM samples, and the LM samples prepared with the NGF-technique and the SVV-technique, respectively. In these figures, the first column shows a lateral cross section, and the second column a cutaway perspective view, both with dense regions being bright. The third column gives an inverted-contrast visualization of the porous structures. In the fourth column, an estimate of the laterally averaged density is given along with the standard deviation.

The FM samples showed binder accumulation regions (dark grey) in the clay. These regions are believed to be zones where the binder (cement and lime) is concentrated as a result of the mixing process. A uniform and constant distribution of these regions might be associated with high strength. Sample RIII-b did not exhibit pronounced dark grey areas, probably associated to the reduced content of binder and therefore the low measured strength. Perhaps the sample was taken from a location where the binder did not mix sufficiently well with the clay, since contrary to the other samples, with the naked eye it was not easy to identify any grey zones. Some small dark black zones were observed with difficulty, which indicate a low presence of entrapped air in the samples, i.e., that the air used in the binder injection was successfully evacuated along the drilling rod as desired during in-situ DDM works.

The LM samples did not show distinct regions of binder accumulation which indicate a good mixture between the clay and the binder. However, the entrapped air was clearly observed when using both moulding techniques. The entrapped air appeared randomly distributed for the SVV-technique and following the compacting layers for the NGF-technique.

3D porosity estimations are believed to be entrapped air resulting from in-situ field installation and laboratory preparation. For the FM samples, porosity was calculated to be 0.5–1.6% (see Table 4), i.e., the volume of voids in relation to the total volume. This is a relatively low value and indicates, as stated above, the successful evacuation of the injected air during field DDM works. The porosity is slightly higher for high α which agrees well with the density values obtained.

For LM however, porosity was calculated to be 6-18 %. Low α yielded large porosity values and a random spreading throughout the sample. In contrast, high α gave low porosity values and a uniform distribution throughout the sample. In both moulding techniques, the cylinder wall friction adds resistance to the compaction efforts creating large pores along the sample edges. The variation of porosity with sample height *z* aims to estimate the porosity of at least two layers by adjusting the reference area between curve extremes. The SVV-technique samples seem to yield a higher porosity overall, especially as compared to the NGF-technique samples where the porosity seems more stable among the different binder quantities. For both methods, the porosity distribution curves (i.e., the normalized gray value curves) clearly show how the compaction creates internal density variations within the samples, giving reduced porosity at the top of each compacting layer and higher porosity at the bottom of each layer.

The results presented above indicate that the current standard laboratory moulding techniques used in Norway have limited ability to represent the field conditions of LC improved clay (i.e., high density, low porosity, and high strength). The LM mixed samples are affected by high α resulting in poor moulding and high porosity. This has an effect on the strength of the improved clay since the failure plane during UC tests tends to follow the pore network inside the sample (i.e., zones with higher porosity act as weak zones in the sample). Since for the NGF-technique, the largest porosity is found in lateral planes coinciding with the compaction layers, there is less impact on the obtained strength and therefore this technique seems to be better at reproducing the field properties. However, the porosity is only part of the strength definition along with the mixing quality and the binder quantity. Recent optimization has shown that the moulding techniques can be improved significantly (Hove et al. 2022).

Conclusions

Two methods frequently used in Norway for preparation of LM-LC improved clay samples have been studied and compared to FM-LC samples using physical and microstructural characterization by µCT-imaging. The use of µCT is a promising tool for reliable characterisation of internal structures, including porosity, in LC-improved clays, that can help explain their mechanical properties.

The FM samples show clear regions of binder accumulation related to the large variation in strength and stiffness in the same column, as well as between columns. In general, columns with low binder contents seem to be more heterogeneous than columns with higher binder contents. These samples show lower porosity values, higher strength, and stiffness than the LM samples. The SVV-technique produces LM samples with lower strength and stiffness, and higher porosity compared to the NGF-technique. With this, it is demonstrated that the current Norwegian laboratory moulding techniques fail to reproduce specimens that are representative for field conditions.

Acknowledgements

The authors would like to acknowledge Hæhre Entreprenør and Nye Veier for allowing sampling at Holvegen, Franzefoss Minerals for sharing the lime material used in the present study and the National Public Road Administration of Norway for partially funding the µCT tests. We thank the Norwegian Research Council for financial support through the projects PoreFlow (#301132), 4D-CT (#275182) and Green sOil stAbiLisation (GOAL, #328767).

List of notations

E_{50}	is the secant Youngs' modulus [kPa]
q_{uf}	is the maximum vertical stress at failure from UC tests [kPa]
UC	is the Unconfined Compression
w_n	is the water content of the improved clay [%]
α	is the binder content, mass of dry binder per m^3 of soil [kg/m^3]
ε_f	is the strain at failure [%]
ρ_{stab}	is the bulk density of improved clay [g/cm^3]
$\tau_{max,\ 28\ d}$	is the maximum shear strength from UC tests ($q_{uf}/2$) [kPa] at 28 days of curing

Accepted manuscript doi:
10.1680/jgele.22.00067

References

Bache B., Wiersholm P., Paniagua P., Emdal A., 2021. Effect of temperature on the strength of lime-cement stabilized Norwegian clay. Journal of Geotechnical and Geoenvironmental Engineering. Accepted for publication.

Bellato, D., Marzano, I.P., Simonini, P., 2020. Microstructural analyses of a stabilized sand by a deep-mixing method. J. Geotech. Geoenviron. Eng. 146(6), 04020032.

Broms, B., 2004. Lime and lime/cement columns. In Ground Improvement. Eds. Moseley M.P. and Kirsch K., Spon Press, Second Edition.

Bruns, S., Stipp, S. L. S. & Sørensen, H. O. 2017. Looking for the Signal: A guide to iterative noise and artefact removal in X-ray tomographic reconstructions of porous geomaterials. Adv. Water Resour. 105: 96–107.

Chavez Panduro, E.A., Cordonnier, B., Gawel, K., Børve, I., Iyer, J., Carroll, S.A., Michels, L., Rogowska, M., McBeck, J.A., Sørensen, H.O., Walsh, S.D.C., Renard, F., Gibaud, A., Torsæter, M., Breiby, D.W. 2020. Real Time 3D Observations of Portland Cement Carbonation at CO2 Storage Conditions. Environmental Science & Technology 2020 54 (13), 8323-8332

Cnudde, V., Boone, M.N. 2013. High-Resolution X-Ray Computed Tomography in Geosciences: A Review of the Current Technology and Applications. Earth-Science Reviews 123: 1-17.

Falle, F., 2021. Comparing laboratory and field stabilised clay. Master's thesis, Norwegian University of Science and Technology, Trondheim, Norway.

Feldkamp, L. A., Davis, L. C. & Kress, J. W. 1984. Practical cone-beam algorithm. J. Opt. Soc. Am. A vol. 1

Hov, S., Falle, F., Paniagua, P. 2022. Optimization of laboratory molding techniques for Nordic dry deep mixing. Geotechnical Testing Journal 45(4): 20210245.

Hov, S., Paniagua, P., Sætre, C., Rueslåtten, H., Størdal, I., Mengede, M., Mevik, C. 2022. Lime-cement stabilisation of Trondheim clays and its impact on carbon dioxide emissions. Soils and Foundations 62 (3): 101162

Jacobson, J.R., Filz, G.M., Mitchell, J.K., 2003. Factors affecting strength gain in lime-cement columns and development of a laboratory testing procedure. Report No. FHWA/VTRC 03-CR16, Virginia Transporation Research Council. Charlottesville, U.S.A.

Jiang, N.-J., Du, Y., Liu, S.,Wei, M.L, A, A. 2016. Multi-scale Laboratory Evaluation of the Physical, Mechanical and Microstructural Properties of Soft Highway Subgrade Soil Stabilized with Calcium Carbide Residue. Canadian Geotechnical Journal. 53: 373-383.

Karlsrud, K., Eggen, A., Nerland, Ø., and Haugen ,T., 2015. Some Norwegian experiences related to use of dry-mixing methods to improve stability of excavations and natural slopes in soft clay. In: Proc. Deep Mixing 2015, San Francisco, DFI, pp. 87–100.

Kitazume, M. & Terashi, M., 2013. The Deep Mixing Method. Taylor & Francis Group.

Kitazume, M., 2005. State of practice report – field and laboratory investigations, properties of binders and stabilized soils. In Proc. International Conference on Deep Mixing – Best Practice and Recent Advances, Stockholm, Sweden, Vol.2, pp.660-684.

Kitazume, M., 2012. Influence of specimen preparation on unconfined compressive strength of cement-stabilized kaolin clay. Proceedings of the International Symposium on Recent Research, Advances and Execution Aspects of Ground Improvement Works, Brussels, Belgium, vol. 2, pp. 385–393.

Accepted manuscript doi:
10.1680/jgele.22.00067

Kitazume, M., Grisolia, M., Leder, E., Marzano, I.P., Alberto, A, Correia, S., Oliviera, P.V., Åhnberg, H., Andersson, M., 2015. Applicability of molding procedures in laboratory mix tests for quality control and assurance of the deep mixing method. Soils and Foundations 55(4):761-777.

Larsson, S., 2003. Mixing processes for ground improvement by deep mixing. Doctoral thesis, KTH Royal Institute of Technology, Stockholm.

Larsson, S., 2021. The Nordic dry deep mixing method: best practices and lessons learned. Keynote lecture. In: Conf. Proc. of Deep Mixing 2021: Best practices and legacy, DFI.

Larsson, S., Dahlström, M., Nilsson, B., 2005. Uniformity of lime-cement columns for deep mixing: a field study. Ground Improvement 9, No.1, pp.1-15.

NGF, 2012. Veiledning for grunnforsterkning med kalksementpeler [In Norwegian]. Norsk geoteknisk forening (Norwegian Geotechnical Society).

SVV, 2016. Statens Vegvesen, Handbook R210 Laboratory investigations [In Norwegian].

Taylor, H. F. W., 1997. Cement Chemistry. Thomas Telford.

Viggiani, G., Hall, S. A. 2012. Full-field measurements in experimental geomechanics: historical perspective, current trends, and recent results. In Advanced experimental techniques in geomechanics (Viggiani, G., Hall, S. A. & Romero, E. (eds)).Grenoble: ALERT Geomaterials, pp. 3–68.

Åhnberg, H., Holm, G., 2009.Influence of laboratory procedures on properties of stabilised soil specimens. In: Proceedings of the International Symposium on Deep Mixing and Admixture Stabilization. Okinawa, 6pp.

Åhnberg, H., 2006. Consolidation stress effects on the strength of stabilised Swedish soils. Ground Improvement (10), No. 1, pp.1-13.,

Åhnberg, H., Johansson, S-E., Retelius, A., Ljungkrantz, C., Holmqvist, L., Holm, G., 1995. Cement och kalk för djupstabilisering av jord [In Swedish]. Swedish Geotechnical Institute Report 48, Linköping.

Table 1. Characteristics of the field mixed columns.

Column name	Binder content α (kg/m³)	Retrieval rate (mm/rev)	Rotation speed (rev/min)	Curing time (days)
RI-a	30	37	150	28
RI-b	30	37	147	28
PII	50	20	170	70
RIII-a	80	17	135	28
RIII-b	80	13	138	28

Table 2. Characteristics of the laboratory mixed samples.

Preparation method	Sample name	Binder content, α (kg/m³)	Curing time (days)
NGF	NGF-I	30	28
	NGF-II	50	28
	NGF-III	80	28
SVV	SVV-I	30	28
	SVV-II	50	28
	SVV-III	80	28

Accepted manuscript doi:
10.1680/jgele.22.00067

Table 3. Set-up values for the μCT measurements.

Settings	Field samples	Laboratory samples
Tube voltage	215 kV	225 kV
Current	173 μA	140 μA
Voxel size	45 μm	30-40 μm
Exposure time	1.42 s	1.42 s
Number of projections	3141	3141
Filter	-	2 mm Cu

Table 4. Results from laboratory tests on field and laboratory mixed samples with porosity estimates from the μCT measurements. The uncertainty is about 10% of the quoted porosity values.

Column/Sample name	Water content, w_n (%)	Density, ρ_{stab} (g/cm³)	Maximum shear strength from UC tests , $\tau_{max,\ 28\ d}$ (kPa)	Strain at failure, ε_f (%)	Stiffness, E_{50} (MPa)	Average porosity (%)
RI-a	23	2.1	222	1.3	61	0.5
RI-b	28	2.1	228	0.9	58	0.8
PII	24	2.0	394*	1.3	80	0.9
RIII-a	27	2.0	323	0.9	116	1.6
RIII-b	26	2.0	184	1.5	43	1.6
NGF-I	30	1.8	160	1.7	34	6.9
NGF-II	29	1.8	235	1.2	54	6.3
NGF-III	28	1.8	304	1.7	72	5.9
SVV-I	30	1.7	111	1.7	20	10
SVV-II	27	1.6	145	1.1	34	14
SVV-III	28	1.6	190	0.9	72	18

*value at 70 days of curing. Using the formula proposed by Åhnberg (2006) $q(t)/q_{28} = 0{,}30lnt$, the calculated value for 28 days is 309 kPa.

Figure captions

Figure 1. Cross-sections of FM samples after UC tests. a) Sample RI-b, α = 30 kg/m^3, b) sample RIII-a, α = 80 kg/m^3, and c) sample RIII-b, α = 80 kg/m^3.

Figure 2. Variation of strength with (a) binder content, α, and (b) macro-porosity, n_{macro}. The numbers next to the symbols refer to the binder content. The strength value for the field sample with α = 50 kg/m³ is corrected for 28 days curing time using the formula proposed by Åhnberg (2006) $q(t)/q_{28} = 0{,}30lnt$.

Figure 3. Macro-porosity estimations and μCT images for FM samples. Black regions show pores and air, while gray regions indicate sample materials, see the main text for further explanations. Scalebar: 5 mm. The macro-porosity is presented as normalized average grey value vs. sample height from top (0 mm) to bottom (50 mm) in the region of interest.

Figure 4. Macro-porosity estimations and µCT images for LM samples prepared by the NGF-method. Black regions show pores and air, while gray regions indicate sample materials, see the main text for further explanations. Scalebar: 5 mm. The macro-porosity is presented as normalized average grey value vs. sample height from top (0 mm) to bottom (50 mm) in the region of interest.

Figure 5. Macro-porosity estimations and µCT images for LM samples prepared by the SVV-method. Black regions show pores and air, while gray regions indicate sample materials, see the main text for further explanations. Scalebar: 5 mm. The macro-porosity is presented as normalized average grey value vs. sample height from top (0 mm) to bottom (50 mm) in the region of interest.

Accepted manuscript doi:
10.1680/jgele.22.00067

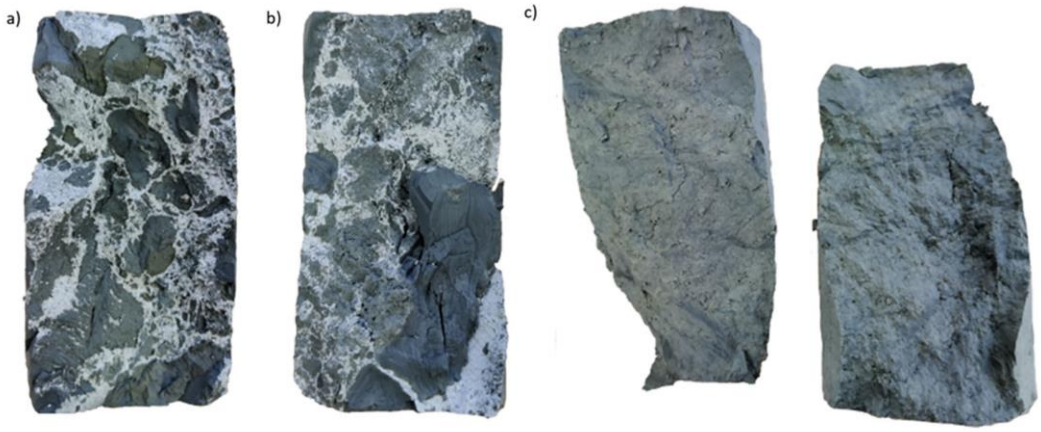

Figure1

Accepted manuscript doi:
10.1680/jgele.22.00067

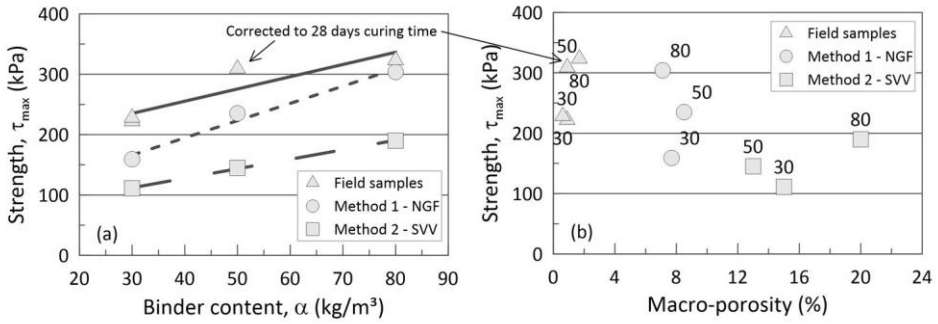

Figure2

Accepted manuscript doi:
10.1680/jgele.22.00067

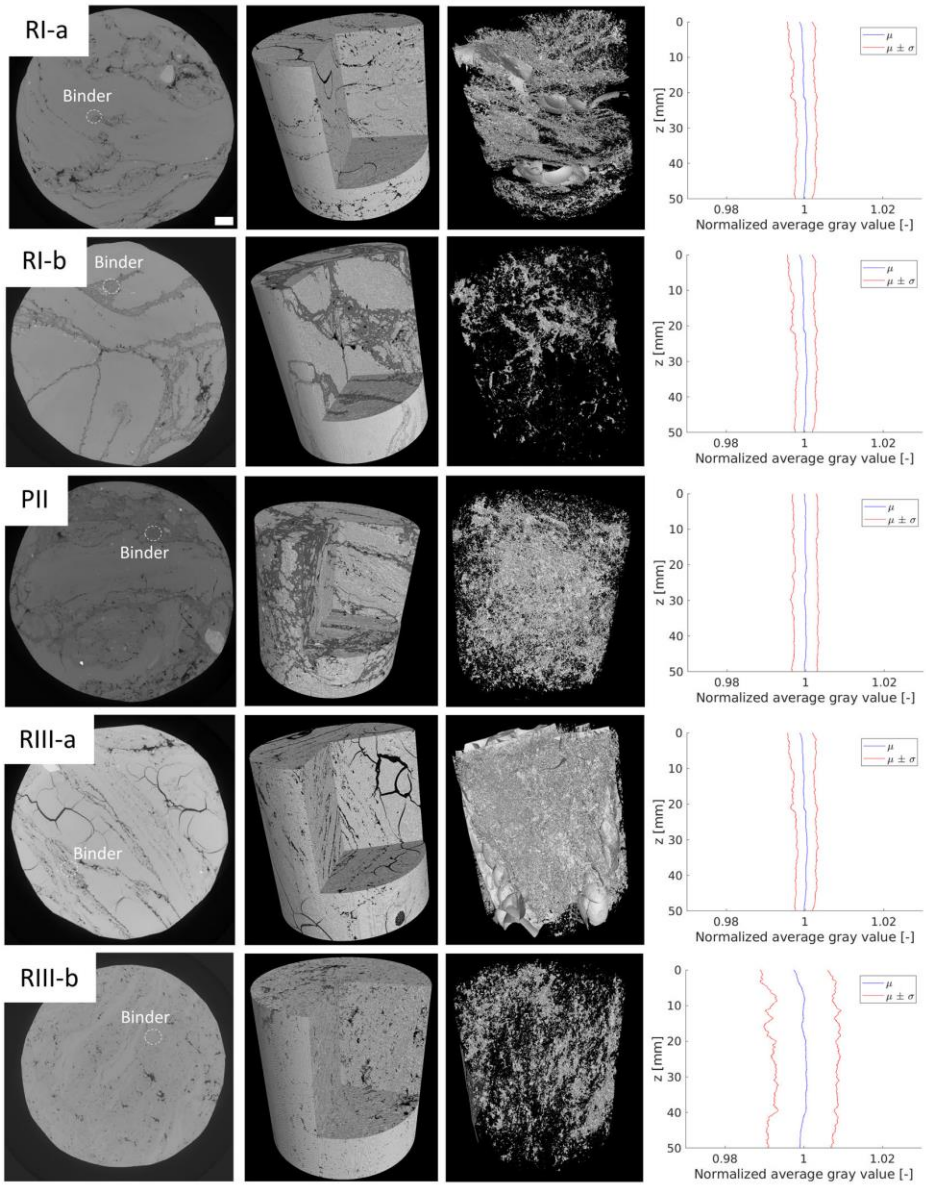

Figure 3

Accepted manuscript doi:
10.1680/jgele.22.00067

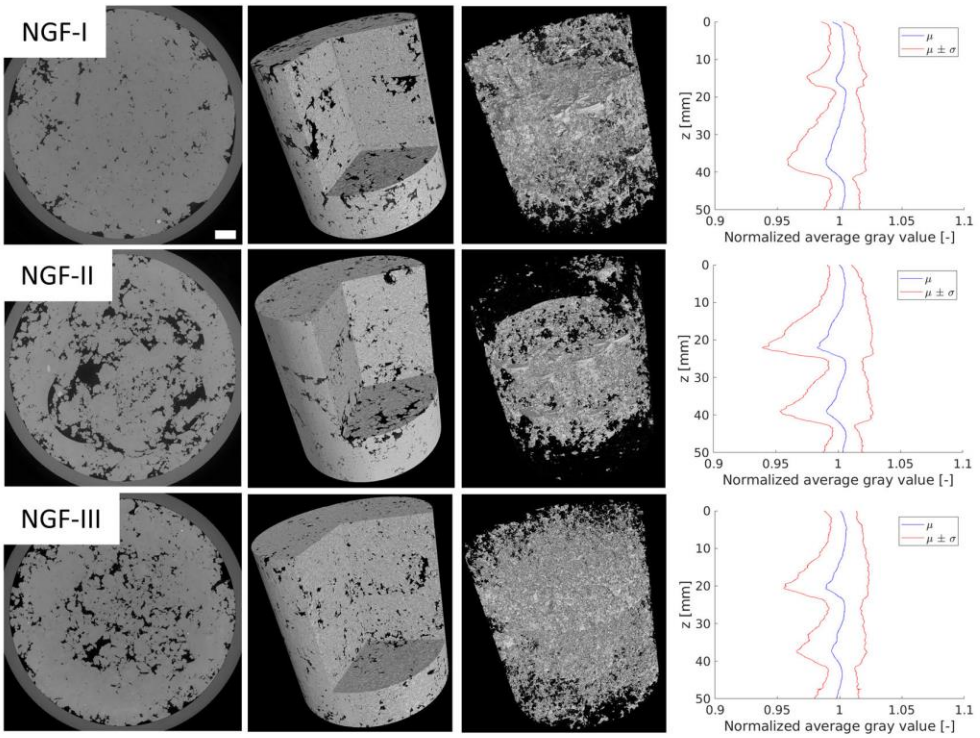

Figure 4

Accepted manuscript doi:
10.1680/jgele.22.00067

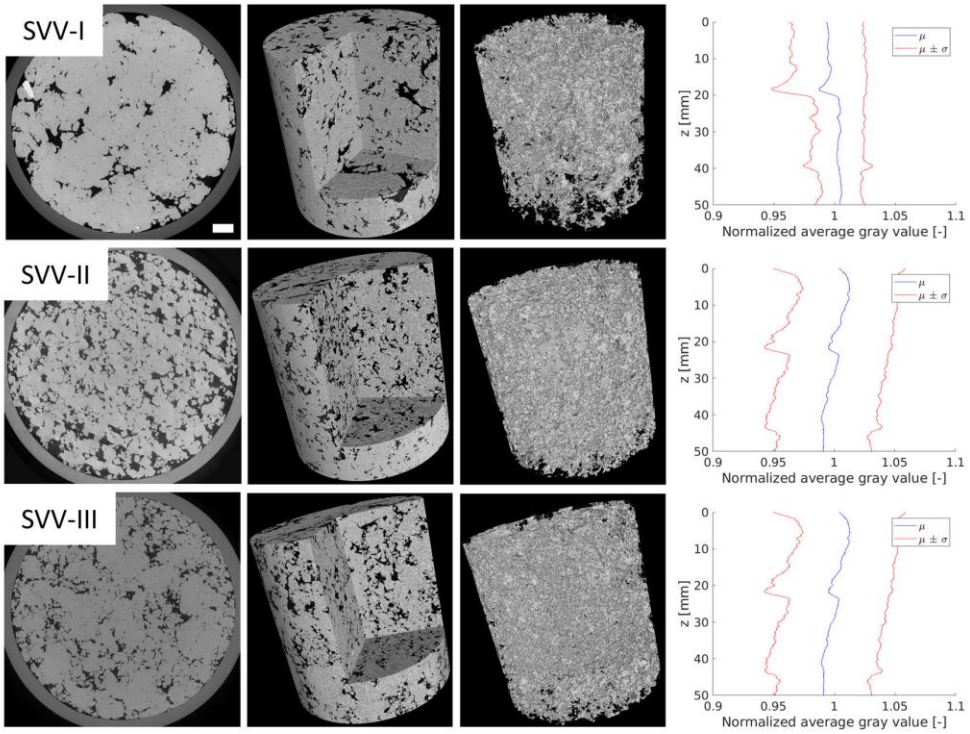

Figure 5